INSPYRE
Investigations Supporting MOX Fuel Licensing in ESNII Prototype Reactors

EERA JPNM
JOINT PROGRAMME ON NUCLEAR MATERIALS

D7.2 – Incorporation and verification of models and properties in fuel performance codes

P. Van Uffelen, A. Schubert (JRC-Karlsruhe), L. Luzzi, T. Barani, A. Magni, D. Pizzocri (POLIMI), M. Lainet, V. Marelle, B. Michel (CEA), B. Boer, S. Lemehov (SCK.CEN), A. Del Nevo (ENEA)

Version 1 – 20/10/2020

The INSPYRE project has received funding from the EURATOM research and training programme 2014-2018 under Grant Agreement No 754329.

Document type	Report
Document number	D7.2 version 1
Document title	Incorporation and verification of models and properties in fuel performance codes
Authors	P. Van Uffelen, A. Schubert (JRC-Karlsruhe), L. Luzzi, T. Barani, A. Magni, D. Pizzocri (POLIMI), M. Lainet, V. Marelle, B. Michel (CEA), B. Boer, S. Lemehov (SCK.CEN), A. Del Nevo (ENEA)
Release date	20/10/2020
Contributing partners	JRC-Karlsruhe, CEA, ENEA, SCK.CEN, POLIMI
Dissemination level	Public

Version	Short description	Main author	WP leader	Coordinator
1	First release	P. Van Uffelen (JRC) 15/10/2020	L. Luzzi (POLIMI) 19/10/2020	M. Bertolus (CEA) 20/10/2020

SUMMARY

This deliverable summarises the first achievements of Task 7.1. The aim of this task was to improve the capabilities of engineering-scale fuel performance codes concerning the simulation of MOX fuel in fast reactor conditions representative of Generation IV systems. This objective was achieved by implementing the mechanistic models developed and recent data on material properties obtained in the other WPs of the INSPYRE Project, but also those available in the open literature and generated by the ESNII+ Project.

The task involved the implementation in the TRANSURANUS, GERMINAL and MACROS codes of models and data concerning

- Mechanical properties: new correlations for the elastic constants and thermal expansion behaviour of MOX fuel for ESNII reactors.
- Thermal properties: new correlations for thermal conductivity and melting temperature of MOX fuels, properly fitted as a function of the relevant parameters.
- Inert gas behaviour: a new model based on a mechanistic approach coupling gas release and swelling.

CONTENT

GLOSSARY

API	Application Program Interface
CMD	Classical Molecular Dynamics
F	Fractional coverage of grain boundary bubbles
FBR	Fast Breeder Reactor
FGB	Fission Gas Behaviour
FIMA	Fissions per Initial Metal Atoms
HBS	High Burnup Structure
HM	Heavy Metal
IDE	Integrated Development Environment
IFPE	International Fuel Performance Experiments
IRSN	Institut de Radioprotection et de Sureté Nucléaire
INSPYRE	Investigations Supporting MOX Fuel Licensing for ESNII Prototype Reactors
KJMA	Kolmogorov-Johnson-Mehl-Avrami
LWR	Light Water Reactor
MA	Minor Actinide
MOX	Mixed Oxide
OECD	Organisation for Economic Cooperation and Development
SEM	Scanning Electron Microscopy
TD	Theoretical Density
WP	Work Package

1 INTRODUCTION

The objective of this document is to summarise the first achievements of Task 7.1. It presents the various models implemented in the three codes considered in the INSPYRE project:

- MACROS [1] developed by SCK.CEN
- TRANSURANUS [2] developed by JRC
- GERMINAL [3] developed by CEA.

The models implemented focus on the three types of properties and phenomena as follows.

- Mechanical properties: new correlations for the elastic constants and thermal expansion behaviour of MOX fuel for ESNII reactors.
- Thermal properties: new correlations for thermal conductivity and melting temperature of MOX fuels, properly fitted as a function of the relevant parameters.
- Inert gas behaviour: a new model based on a mechanistic approach coupling gas release and swelling.

2 IMPROVEMENT OF MACROS

The model improvements considered by SCK.CEN are the implementation of new correlations for the thermal expansion and the Young's modulus of MOX fuel. New correlations were derived for these properties within the INSPYRE Project. These correlations, which are summarized below, are incorporated in the MACROS code (2020 version) of SCK.CEN, and were implemented also with adaptations / modifications) in the TRANSURANUS code (see Section 3.2) and in the GERMINAL code (Section 4.2). These correlations, their development and validation are described in detail the D6.3 Deliverable of the INSPYRE Project [4].

The impact of the novel correlations in comparison with the existing ones is investigated based on the simulation of the RAPSODIE-I irradiation experiment. Details of the implemented correlations and the differences with the state-of-the-art correlations are given below.

2.1 Improved model for thermal expansion

The novel correlation for the linear thermal expansion coefficient reads:

$$\frac{\Delta L}{L_y} = \frac{\Delta L}{L_0}\left[1 + b_y\left(2 - \frac{O}{M}\right)\right] (\%) \quad (1)$$

Where, y corresponds to the deviation from stoichiometry ($1.94 \le O/M \le 2.00$) and

$$\frac{\Delta L}{L_0} = b_0 + b_1 \cdot \frac{T}{T_M} + b_2 \cdot \left(\frac{T}{T_M}\right)^2 + b_3 \cdot \left(\frac{T}{T_M}\right)^3 \quad (\%) \quad (2)$$

$$T_M = T_{UO_{2.00}}^{(m)} \times (1-x) + x \times T_{PuO_{2.00}}^{(m)} \quad for\ x \le 60\%Pu \quad (3)$$

Where, T is the temperature in K, T_M is the melting temperature in K, x is the fraction of Pu/HM and all the numerical parameters of the correlations and the associated uncertainties are listed in Table 1.

Parameter	Value	Error (±)
b_0	-0.3080	0.0260
b_1	3.4303	0.1889
b_2	-1.9157	0.3977
b_3	3.4636	0.2497
b_y	3.98	--
$T_{UO_{2.00}}^{(m)}$ (Best Estimate)	3127	33
$T_{PuO_{2.00}}^{(m)}$ (Best Estimate)	2804	33
$T_{UO_{2.00}}^{(m)}$ (Conservative)	3101	43
$T_{PuO_{2.00}}^{(m)}$ (Conservative)	2649	43
$1\sigma\left(\frac{\Delta L}{L_0}\right)$	0.0412	--
$1\sigma\left(T_M\right)$	16	--

Table 1: List of parameters to be used with the improved MOX thermal expansion correlation.

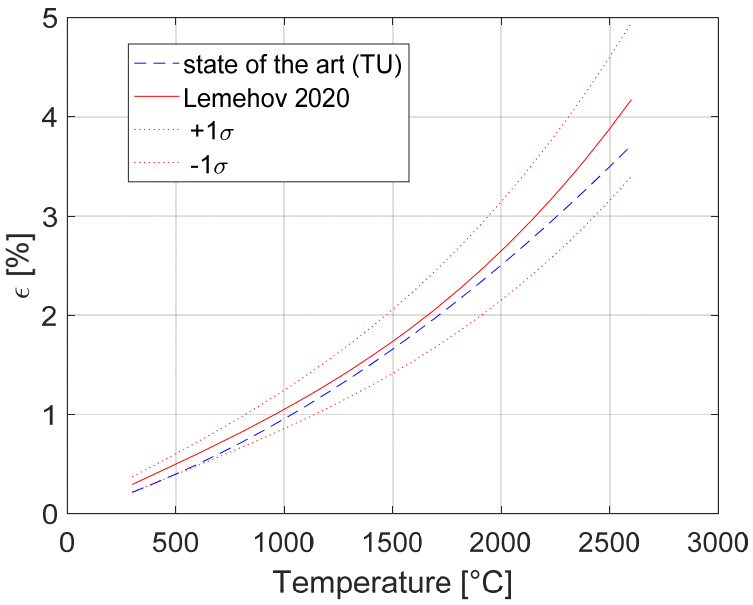

Figure 1: Standard TRANSURANUS correlation for thermal expansion of 30 % MOX fuel with O/M = 1.99, compared to the new correlation developed by S. Lemehov (including ±1σ uncertainty).

A comparison between this correlation and the one used in the TRANSURANUS code for fast reactor MOX applications (e.g., the preliminary simulations of the RAPSODIE-I irradiation performed in INSPYRE) is shown in Figure 1. The new correlation predicts slightly higher thermal expansion than the one employed in the standard TRANSURANUS code version.

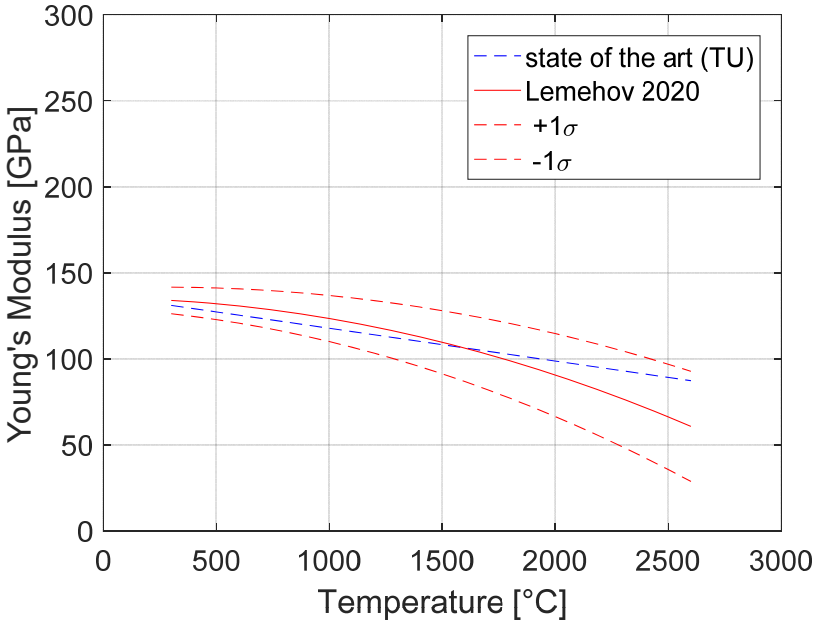

Figure 2: The standard TRANSURANUS correlation (state of the art) for Young's modulus of 30 % MOX fuel with O/M = 1.99 and porosity p = 0.15, compared to the correlation developed by S. Lemehov (including ±1σ uncertainty).

2.2 Updated model for Young's modulus

A novel correlation for the Young's modulus (E, GPa) of MOX fuel as a function of Pu content, porosity, oxygen-to-metal ratio and temperature was developed. In summary, the equations composing the proposed model are:

$$E_{MOX,0}(x) = (1 - x) \times E_{UO_{2.00}} + x \times E_{PuO_{2.00}} \quad (4)$$

with x representing the Pu/HM fraction, $E_{UO_{2.00}}$ = 218.74 ± 1.13, and $E_{PuO_{2.00}}$ = 249.45 ± 1.27.

The stoichiometry is considered using the following relationship:

$$E_{MOX}(y) = E_{MOX,0} + y \times \frac{\partial E}{\partial y} \quad (5)$$

with $y = 2 - O/M$ and $\frac{\partial E}{\partial y}$ = -586 ± 86.95 for $y \leq 0.037$ and $\frac{\partial E}{\partial y}$ = -126.59 ± 40.22 for $y > 0.037$.

The fractional porosity dependency is then introduced as follows:

$$\frac{E(p)}{E_0} = \frac{(1-p)^2}{1 + p \cdot A_E} \quad (6)$$

with A_E = 1.100.

The temperature dependence can be taken into account by fitting directly the experimental data of Martin *et al.* [5], resulting in:

$$\frac{E(T)}{E_0} = b_0 + b_1 T + b_2 T^2 \quad (7)$$

With T in K, b_0 = 0.9796, b_1 = 3.1597 10^{-5}, b_2 = -7.6164 10^{-8}.

A comparison between the new correlation (Eq. (7), including 1σ uncertainty bands) and the standard correlation used in TRANSURANUS (for 30 % Pu-MOX with O/M = 1.99) is shown in Figure 2. The new correlation predicts a similar Young's modulus as the original one used in the code, although it gives lower values at high temperature (17 % lower at T > 2300°C).

3 IMPROVEMENT OF TRANSURANUS

3.1 Thermal properties

In the PhD of A. Magni, novel physically grounded or semi-empirical models correlations for the thermal conductivity and melting temperature of fast reactor MOX considering all the fundamental parameters (i.e., fuel temperature, burn-up, plutonium content, deviation from stoichiometry, porosity) were developed by the fit of recent and reliable experimental data. These new correlations were statistically assessed through a p-value analysis, which confirmed the need for the inclusion of all the parameters above in both models.

These correlations, their development and validation are described in detail both in the version 2 of the D6.2 Deliverable of the INSPYRE Project [6] and in a publication in the Journal of Nuclear Materials [7]. We recall here only their functional forms and parameters as implemented in the code.

3.1.1 Thermal conductivity

The correlation for thermal conductivity of fresh fast reactor MOX reads [7]:

$$k_0(T,x,[Pu],p) = \left(\frac{1}{A_0 + A_x \cdot x + A_{Pu} \cdot [Pu] + (B_0 + B_{Pu}[Pu])T} + \frac{D}{T^2} e^{-\frac{E}{T}}\right)(1-p)^{2.5} \quad (8)$$

and the corresponding correlation for irradiated MOX is

$$k_{irr}(T,x,[Pu],p,bu) = k_{inf} + (k_0(T,x,[Pu],p) - k_{inf}) \cdot e^{-\frac{bu}{\varphi}} \quad (9)$$

The variables and fitted parameters of the correlations are given in the following tables.

Variable	Units	Meaning
T	K	Temperature
[Pu]	at /	Plutonium content
x	-	Deviation from stoichiometry (2.0 - O/M)
p	TD /	Porosity
bu	GWd/tHM	Burn-up
k_0	W/(m·K)	Thermal conductivity of fresh fuel
k_{irr}	W/(m·K)	Thermal conductivity of irradiated fuel

Table 2: Variables in the new correlation for the thermal conductivity of MOX.

Regressor	Units	Estimate
A_0	m·K/W	0.01926
A_x	m·K/W	$1.06\ 10^{-6}$
A_{Pu}	m·K/W	$2.63\ 10^{-8}$
B_0	m/W	$2.39\ 10^{-4}$

B_{Pu}	m/W	$1.37\ 10^{-13}$
D	W·K/m	$5.27\ 10^{+9}$
E	K	17109.5
k_{inf}	W/(m·K)	1.755
φ	GWd/tHM	128.75

Table 3: Parameters of the new correlation for the thermal conductivity of MOX.

The validity ranges have been extended with respect to state-of-the-art correlations and correspond to the ranges covered by the experimental data used for the fitting:

- Temperature, T: [500, 2700] K.
- Deviation from stoichiometry, *x*: [0, 0.04] (hypo-stoichiometry).
- Plutonium content, [Pu]: [0, 45] wt.%.
- Porosity, p: [0, 7] %.
- Burn-up, bu: [0, 130] GWd/tHM.

3.1.2 Melting temperature

The derived correlation for the fresh fast reactor MOX fuel melting (or solidus) temperature (in K) is given by (see reference [7]):

$$T_{m,0}([Pu], x) = T_{m,UO_2} - \gamma_{Pu}\,[Pu] - \gamma_x\, x \tag{10}$$

While the correlation for the melting temperature (K) of irradiated MOX reads

$$T_{m,irr}(bu, [Pu], x) = T_{m,inf} + (T_{m,0}([Pu], x) - T_{m,inf}) \cdot e^{-\frac{bu}{\delta}} \tag{11}$$

Where, the variables are the same defined as above and the fitted parameters are listed in the table below:

Regressor	Units	Estimate
$T_{m,UO2}$	K	3147
γ_{Pu}	K / at./	364.85
γ_x	K	1014.15
$T_{m,inf}$	K	2964.92
δ	GWd/tHM	40.43

Table 4: Variables and fitted parameters of the new correlation for the melting temperature of MOX.

The validity ranges have been extended with respect to state-of-the-art correlations and correspond to the ranges covered by the experimental data used for the fitting:

- Deviation from stoichiometry, *x*: [0, 0.06] (hypo-stoichiometry).
- Plutonium content, [Pu]: [0, 50] wt.%.
- Burn-up, bu: [0, 110] GWd/tHM.

The novel MOX thermal conductivity and melting temperature correlations were implemented in the TRANSURANUS fuel performance code (both versions v1m1j18 and v1m1j20), for validation against integral data from the HEDL P-19 irradiation experiment, concerning MOX fuel in fast reactor start-up conditions. The new correlations show a promising predictive capability of both integral and local experimental data from post-irradiation examinations, improving or at least matching the predictions

from state-of-the art correlations. The code calculations are generally conservative with respect to the experimental measurements, since the power-to-melt is under-estimated, and the fuel axial and radial melting extents are over-estimated.

This work represents a step towards the extension, improvement and validation of fuel performance codes for application to safety analyses on fast reactor MOX fuel, which are of great interest for the development of Generation-IV reactor concepts. Additional experimental measurements and uncertainty indications will help to both further improve and validate the novel models herein presented, along with data assimilation techniques. As a complement, values calculated using Molecular Dynamics simulations could further support and interpret experimental data. As a potential future model improvement, the development of a mechanistic approach to thermal conductivity is of great interest to increase the physical ground of the model developed in this work. To this end, one could consider either the fission product concentration remaining in the fuel or an effective fuel burnup to include the effect of annealing of the irradiation damage and fission product removal at high temperatures (typical for fast reactor MOX) in the model. Moreover, this kind of approach would be applicable to other nuclear fuel materials (e.g., minor actinide-bearing fuels) and thermal properties (e.g., thermal diffusivity, heat capacity).

3.2 Mechanical properties

The mechanical properties considered (thermal expansion and Young's modulus for MOX) were derived from the routines developed by SCK.CEN. The correlations are described in detail in the version 2 of the D6.3 Deliverable of the INSPYRE Project [4]. The implementation of the material properties in the TRANSURANUS code was finalized at JRC. More precisely, the initial draft version of the driver routines eloc.f90 and thstr.f90 provided by SCK.CEN were reprogrammed as follows.

First, both material properties were reprogrammed in a specific subroutine, which is in line with the general code structure, and were tested in the separate standalone environment for development of models in TRANSURANUS. The effect of the stoichiometry described in Section 2 below was also included on the basis of the variables available in the TRANSURANUS code (ozum3). The atomic fraction of Pu was also expressed on the basis of the variables available in the TRANSURANUS code (cnpu3). The correlation for the thermal expansion coefficient makes use of the material-specific melting temperature provided in the code. For the sake of consistency, the code user should thus invoke the new correlation for the melting temperature developed by A. Magni summarized in Section 3.1 and described in detail in D6.2 v2 [6] and [7], in order to take into account the effects of varying composition (Pu, O/M, burnup, etc.) on the phase transition.

As far as the temperature effect on the elastic modulus is concerned, a further modification was made to clarify some of the differences revealed in Figure 3. This figure compares the elastic modulus for fully dense and fresh MOX fuel with 30 % Pu content as a function of the temperature, obtained with various correlations:

- TU standard: The standard correlation for Young's modulus included in the TRANSURANUS code [2].
- SCK.CEN: The correlation for Young's modulus proposed by SCK.CEN in Task 6.2 (see Section 2.2 above, with the temperature dependency described therein), and included in D6.3.
- Hirooka: The original correlation for Young's modulus derived by SCK.CEN in Task 6.2 on the basis of data of Hirooka *et al.* [8].
- MATPRO: The SCK.CEN correlation for Young's modulus, but with the temperature dependency in accordance with the MATPRO library [9], which is largely used in fuel performance calculations.
- ESNII+: The SCK.CEN correlation for Young's modulus, but with the temperature dependency in accordance with the more recent ESNII+ review report [10].

- TU (new): The SCK.CEN correlation for Young's modulus, but with the temperature dependency of Equations 12 and 13 derived from the molecular dynamics calculations of Balboa *et al*. [11] in the INSPYRE Project.

SCK.CEN performed a comprehensive work, proposing equations for thermomechanical properties of Pu containing mixed-oxide fuel including their dependencies on temperature, Pu content, O/M ratio and porosity. The results are collected in the INSPYRE deliverable D6.3. The SCK.CEN correlation derived for the elastic modulus largely relies on the recent experimental work of Hirooka *et al*. [8], who measured sound speeds of longitudinal and transverse waves in the uranium–plutonium mixed oxide pellets with varying degrees of porosity, oxygen-to-metal ratio, and plutonium content. The effect of each parameter was well fitted by a linear function, although the temperature dependency had to be inferred by calculations. The discussion of Hirooka *et al*. about their temperature dependency (Figure 8 in [8]) indicates room for further research. On the one hand, they suggest that the data of Padel *et al*. [12] are better in terms of temperature dependency because measured at different temperatures, unlike Hirooka *et al*. who carried out measurements only at room temperature. On the other hand, they mention that the data of Padel *et al*. are inaccurate and conclude that the accuracy of the data in the high temperature region needs to be further investigated. The curve calculated by Hirooka and co-workers, however, is in line with the review and conclusions of Ottaviani *et al*. in the ESNII+ Project [10], who proposed a polynomial function of second order to express the Young's modulus dependence on temperature. Similarly, SCK.CEN proposes a second order polynomial by fitting the data used in the ESNII+ Project (see Section 2.2), i.e., by fitting directly the experimental data of Martin *et al*. [5]. The standard correlation in TRANSURANUS, proposed by Lassmann *et al*., as well as the more recent MATPRO correlation, were simpler in form (i.e., linear correlations).

In Task 3.1 of the INSPYRE Project, Balboa *et al*. [11] performed classical molecular dynamics (CMD) calculations that can complement experimental data, especially in the high temperature region. The interatomic potentials of Cooper *et al*. [13] used in the CMD calculations were fitted to experimental data at room temperature but provide a temperature dependency of the elastic modulus that is very well in agreement with the recent review of the ESNII+ Project. The CMD calculations analysed both the effect of plutonium content and temperature. The effect of the plutonium content is small and hard to distinguish in the scatter of data yielded by the statistical analysis. The dependence of CMD data on the temperature was fitted using a second order polynomial, in line with the ESNII+ report. The temperature dependent function as follows was obtained:

$$f(T) = E_1 + E_2 \cdot T + E_3 \cdot T^2 \tag{12}$$

where, T represents the absolute temperature (K), E_1 = 219.12, E_2 = -0.0154, and E_3 = $-9.0 \cdot 10^{-6}$.

The expression of the Young's modulus E_T as a function of temperature in Figure 21 of Deliverable D6.3 is then replaced in TRANSURANUS by the correlation as follows:

$$E_T = E_{MOX} \frac{f(T)}{f(273K)} \tag{13}$$

where, we normalised the CMD results at 273 K and E_{MOX} is given by Eq. 5 in Section 2.2. As shown in Figure 3, the result is very similar to that proposed by the ESNII+ Project and by SCK.CEN. There is mainly an increasing over-prediction towards the melting temperature, which is however smaller than the experimental uncertainty as well as the scatter in the CMD results. The resulting expression for the elastic modulus, which combines the thermodynamic analysis performed by SCK.CEN with the molecular dynamics calculations of Balboa *et al*. [11] is therefore proposed as new correlation to be used by TRANSURANUS for the re-assessment in INSPYRE of improved codes.

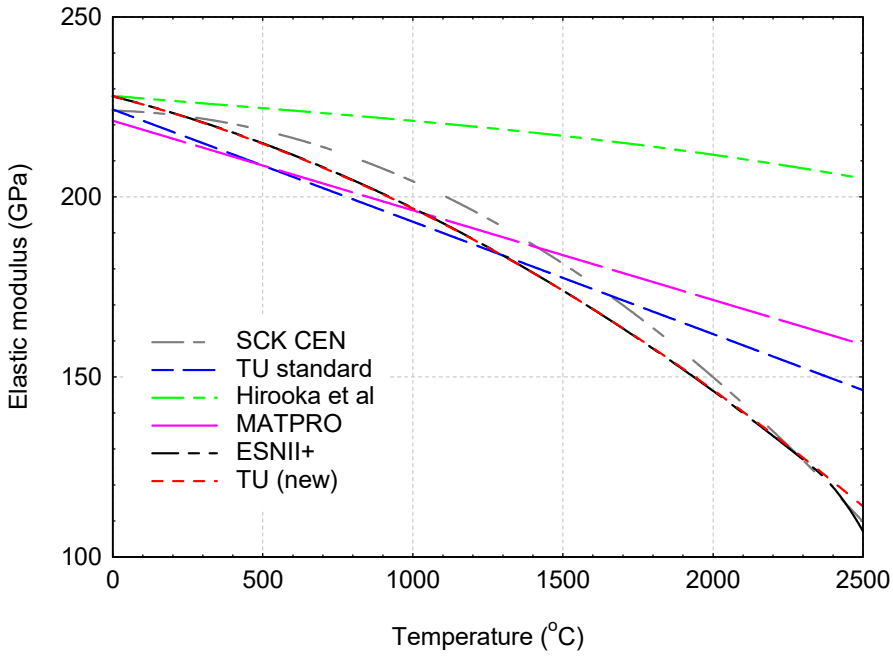

Figure 3: Comparison of the various correlations for the elastic modulus (MPa) with the proposed correlation developed in INSPYRE, for fully dense fresh stoichiometric FBR MOX with and 30 % Pu content, as a function of the temperature (°C). The correlations are described in the text.

Also the possibility to apply uncertainty variations typical for Monte Carlo studies inherently available in the TRANSURANUS code is implemented, and the effect of deviations from stoichiometry on the elastic modulus was integrated on the basis of the formulation given in Section 2.

Finally, the correlation for the thermal expansion of MOX fuel in the solid phase is integrated in a biphasic law that takes into account the volume increase during melting and also evaluates the thermal expansion in liquid phase beyond melting.

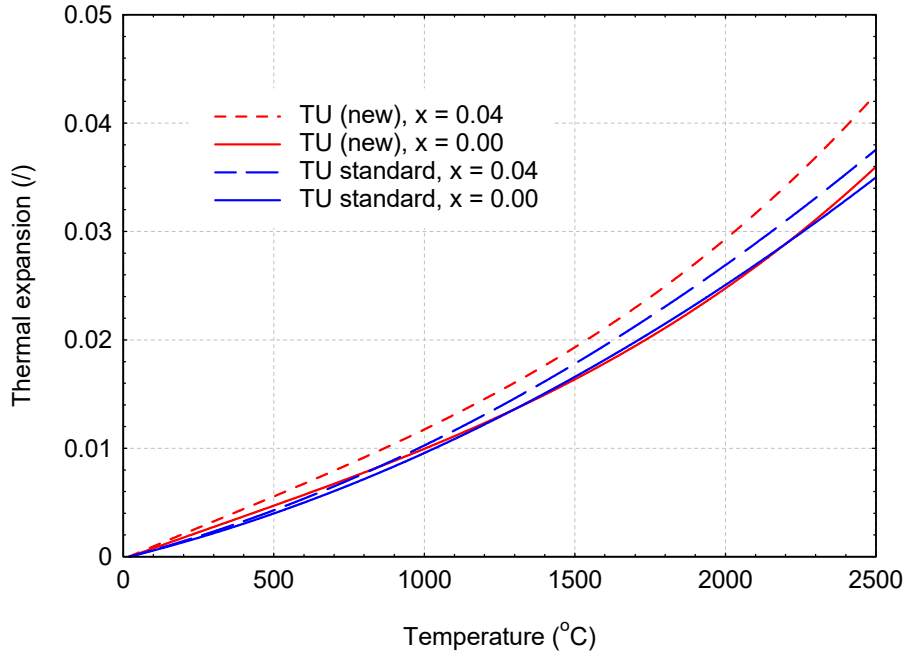

Figure 4: Comparison of the standard correlation of TRANSURANUS for the thermal expansion coefficient with the new proposed correlation developed in INSPYRE, for fresh FBR MOX fuel, as a function of the temperature (°C).

The standard correlation for the thermal expansion in TRANSURANUS is compared with the new INSPYRE version in Figure 4. The standard TRANSURANUS correlation [2] is based on a second order polynomial function of the temperature, which is very similar to that proposed by S. Lemehov in the new correlation for the MACROS code (Section 2.1). The effect of stoichiometry deviation is considered in both the standard and novel correlations by means of a linear correction factor valid for the sub-stoichiometric region. The standard correlation is based on the work of Gibby [14] and uses a factor of 1.83, whereas the new correlation (Eq. 1 in Section 2.1) uses a factor of 3.98, which is based on the more recent data of Martin et al. [5]. The higher correction coefficient for the deviation from stoichiometry in the new correlation is clearly visible in Figure 4, whereas the temperature dependency of both correlations is very similar when considering the experimental scatter of the data.

3.3 Inert gas behaviour

The details of the developments are presented in Deliverable D6.4 of the INSPYRE Project [15]. In the current deliverable, we briefly outline the improvements and provide more information about the implementation in fuel performance codes.

The first mechanistic model for TRANSURANUS deals with the description of intra-granular fission gas behaviour during irradiation. It is a fundamental part of models used for the calculation of fission gas release and gaseous swelling in nuclear fuel performance codes. The relevant phenomena include diffusion of gas atoms towards the grain boundaries coupled to the evolution of intra-granular bubbles. During normal operating conditions, these bubbles are limited to sizes of a few nanometres. Experimental evidence exists for the appearance of a second population of bubbles during transients, characterized by coarsening to sizes of tens to hundreds of nanometres [16]. These can significantly contribute to gaseous fuel swelling. In the PhD work of T. Barani [17, 18], a new model of intra-granular fission gas behaviour in uranium dioxide fuel that includes both nanometric fission gas bubble evolution and bubble coarsening during transients was developed.

In particular, the new model considers the role of dislocations as a source of vacancies, in combination with preferential growth along dislocations as the mechanism for bubble coarsening in the fuel grains during in-pile transients. This theory is supported by experimental observations showing coarsened bubbles associated with dislocations [16, 19-22]. It extends the concept of the established behaviour of defects at grain boundary bubbles to dislocations. More precisely, it is assumed that in high temperature transients, dislocation bubbles absorb vacancies in the dislocation core region when their internal energy (pressure) exceeds the equilibrium value. The model extends previous work [23] on intra-granular bubble evolution that was limited to normal operating conditions. The new model integrates information inferred from molecular dynamics and atomistic calculations in its parameters (e.g., irradiation-induced re-solution and defect diffusivities along dislocation lines). The model therefore combines a mechanistic description of bubble evolution to a limited complexity, which is suited for application in engineering fuel performance codes such as TRANSURANUS.

In view of its verification, the stand-alone model was applied to simulations of local fission gas behaviour for the experimental database by White *et al.* [22], included in the IFPE database [24]. The selected set consists in measurements performed on 12 UO_2 samples of fuel pins irradiated up to a burnup between 9 and 21 GWd t^{-1} in the OECD Halden reactor. After the base irradiation, the pins were either subjected to a power ramp or to power cycles. SEM examinations were then performed at different radial positions.

On the one hand, the comparison to experimental data revealed an overall satisfactory agreement between calculated values and experimental data in terms of both bubble radius and associated gaseous swelling (Figure 5, left). On the other hand, comparisons in terms of bubble number density were less satisfactory. The ramp-tested fuel samples contained intra-granular coarsened bubble of sizes of tens to

hundreds of nanometres and volumetric swelling of one to several percent. These values are orders of magnitude higher than bubbles sizes and swelling observed under normal operating conditions, and could not be reproduced with traditional models that do not include specific transient capabilities. The model is now available to TRANSURANUS via its coupling with the SCIANTIX code (see below). Finally, it should be underlined that the physics-based approach to the description of intra-granular gas behaviour considered in the present model may be applied to other types of oxide fuels, such as plutonium-uranium mixed oxide fuels, both in LWR or FBR conditions. Nevertheless, it is recommended that model parameters will be updated to comply with the specific material and reactor peculiarities, when appropriate experimental data become available.

A second important mechanistic model concerning fission gas behaviour in oxide fuels was developed, which relates to the so-called High Burnup Structure (HBS) that was first observed in FBR MOX fuels and later in LWR fuels. Local high irradiation damage at low temperatures triggers a restructuring in the original microstructure of nuclear fuels, leading to the formation of this HBS. It affects the integral behaviour of the nuclear fuel pin in both normal operating and accident conditions. Therefore, fuel performance codes need to incorporate proper models accounting for HBS effects. In the PhD of T. Barani [17], a new model describing the HBS formation and the progressive intra-granular xenon depletion in UO_2 was also proposed. The HBS formation is modelled employing the Kolmogorov-Johnson-Mehl-Avrami (KJMA) formalism for phase transformations. The coefficients of the KJMA correlation were fitted to experimental data on the restructured volumetric fraction as a function of the local effective burnup. To this end, available experimental data [25], together with novel data extracted from a recent publication [26], were used.

For its verification, the HBS formation model is coupled to a description of the intra-granular fission gas behaviour in the SCIANTIX code (see below), allowing us to estimate the evolution of the retained xenon in order to compute consistently the fission gas retention in the matrix and its effect on the fuel swelling (see refs [17, 27]).

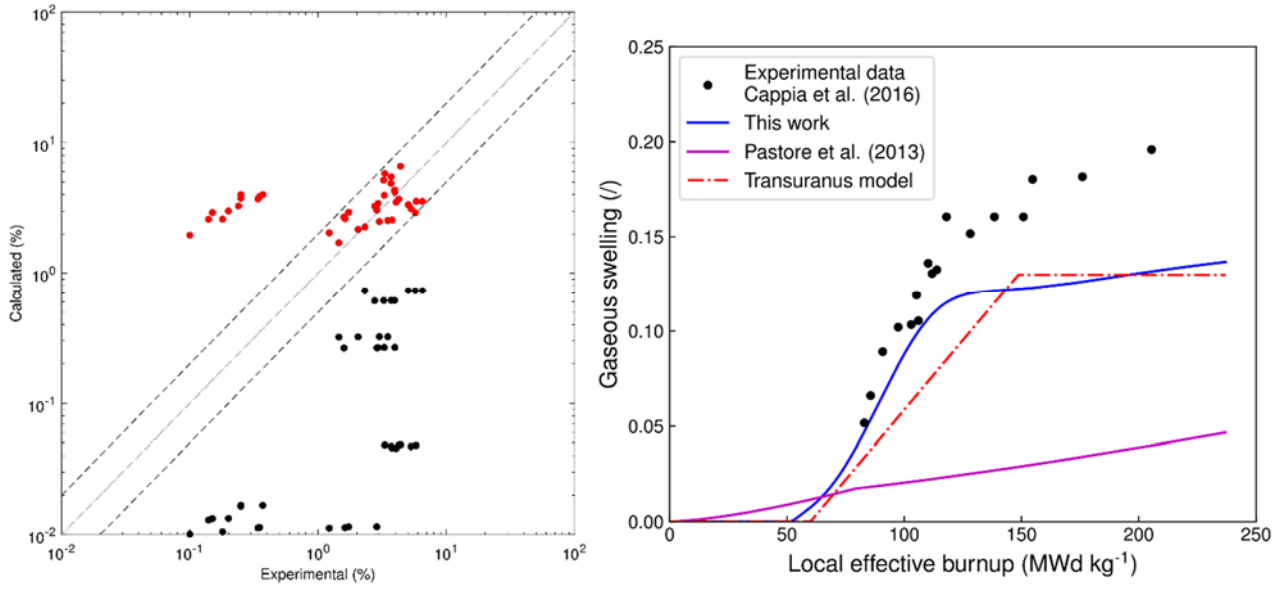

Figure 5: Left: Comparison of the calculated (red marks with the new intra-granular coarsening model [18], black marks with the model for only nanometric intra-granular bubbles [10]) to experimental data on intra-granular gaseous swelling from the experimental database of White [4]. Right: Comparison between calculated and experimental HBS swelling on the experimental database by Cappia *et al.* [8]. The predictions in solid purple are calculated with the simple model from the literature for inter-granular gaseous swelling, also available in SCIANTIX (Figures taken from [28]).

The model predictions were compared to experimental data and state-of-the-art models' results, including for example the empirical model in the basic version of the TRANSURANUS code, in terms of porosity, xenon depletion and fuel matrix swelling as a function of the local burnup. As an illustration, the evolution of porosity as a function of local burnup is shown in Figure 5 right. The satisfactory agreement paves the way to the inclusion of the model in fuel performance codes [28].

As a third component of the modelling of inert gas behaviour in oxide fuel, a new mechanistic model for helium behaviour [29] was developed in the PhD of L. Cognini. In a similar way as for fission gas, the model includes single-atoms diffusion in an equivalent sphere, trapping of single atoms at intra-granular bubbles, irradiation induced re-solution of gas atoms from intra-granular bubbles and the helium production rate. However, unlike the model for fission gas, also the helium solubility is taken into consideration. Important model parameters such as solubility [30] and mobility [31] was inferred from an extensive review in combination with a set of new experiments at the JRC, whereas the correlation suggested by Van Brutzel *et al*. [32] was implemented as equation of state for the intra-granular bubble pressure. In order to account for the effect of grain growth and the consequent grain boundary sweeping, the Van Uffelen *et al*. grain growth model [33] was applied.

In the verification process and comparison of model predictions with experimental data, two models are considered, i.e., the current model available in TRANSURANUS and the new mechanistic model. Both models are implemented in SCIANTIX (see below). The experimental data considered are annealing tests by Talip *et al*. performed in vacuum conditions at different temperatures [34], to investigate the helium release from UO_2 samples (doped with 0.1 wt.% of additive containing 66.7 wt.% of $^{238}PuO_2$, aged 15 years). The five annealing temperature histories considered are characterized by a heat-up step of around 30 minutes (with heating rate of 10-30 K min^{-1}), followed by a holding time at the annealing temperature for 1-3 hours. In three out of five annealing histories, the temperature is decreased after the plateau, while in two histories a second heat up phase up to 2200-2300 K was carried out. For each temperature history, two figures of merit were analysed, namely: the helium fractional release and the helium release rate. The helium fractional release is measured up to the end of the annealing plateau, while the helium release rate is measured continuously to the end of the annealing history (i.e., for two cases, up to 2200-2300 K).

The agreement between the results of the new mechanistic model and the experimental data is overall satisfactory, and proves that the new mechanistic model is equivalent with the current semi-empirical model in TRANSURANUS. The remaining differences have been ascribed to either a missing additional mechanism (such as intra-granular bubble mobility) and/or a poor characterisation of some model parameters. A closer analysis enabled to isolate the model parameters responsible for the discrepancy between predictions and experimental results, namely, the activation energy of the thermal re-solution of helium from intra-granular bubbles.

It is worth stressing that besides its currently limited predictive capabilities in specific cases, the new mechanistic model has the inherent potential capability to reproduce the main physical phenomena observed in the experiments considered. Moreover, given the mechanistic formulation of the new proposed model, it will be possible to include directly new parameters as they become available, either from lower-length scale calculations as for the intra-granular bubble behaviour model of SCIANTIX presented above, or from dedicated experiments. Furthermore, the mechanistic approach, which is also adopted in the MFPR-F code for example [35], is suitable to combine the models for the inert fission gases and helium in irradiated fuels that are integrated in SCIANTIX.

Finally, Pizzocri *et al*. developed the SCIANTIX code [36], a dedicated intermediate-scale code in order to bridge lower length-scale calculations with the engineering-scale simulations of fuel performance codes. It is an open source 0D stand-alone computer code designed to be included/coupled as a module

in existing fuel performance codes like TRANSURANUS. The version of SCIANTIX tailored for INSPYRE contains [28, 36, 37]:

- A description of helium behaviour based on the treatment of fission gas behaviour but including additional terms, such as the solubility [30, 38-40].
- A description of actinide evolution with burnup, based on a reduced order model employing Bateman's equations with energy-averaged cross sections considered as functions of burnup and initial fuel composition [41-43]. This depletion capability implies the prediction of the helium production rate.
- A model describing intra-granular bubble coarsening, considering an additional growth mechanism for bubbles attached to dislocations [18, 22].
- A model describing the venting of inter-granular bubbles [44].
- A model describing the development of the HBS [27].
- A reduced order model describing the diffusion of intra-granular gas in columnar grains [45], relevant for the simulation of MOX fuel in fast reactor conditions.

Longer-term developments include the description of fission product formation and evolution, and the description of point defect evolution and interaction with fission gas, in a similar way as in the MFPR-F code. For all these model developments, the validation strategy based on comparison with separate-effect experiments is going to be applied when possible. As for the inclusion of SCIANTIX within fuel performance codes as a fission gas behaviour module, the current status is that the coupling was demonstrated in TRANSURANUS [37] and will be the subject of future publications, was achieved for GERMINAL code [3] in the INSPYRE Project and is being pursued for the FRAPCON code in the R2CA Project.

4 IMPROVEMENT OF GERMINAL

The GERMINAL code was improved by integrating in the code:

- New correlations for MOX thermal conductivity, heat capacity and melting temperature
- New correlations for MOX thermal expansion and Young's modulus
- The SCIANTIX inert gas behaviour model.

4.1 Thermal properties

4.1.1 Thermal conductivity

The correlation for thermal conductivity presented in Section 3.1.1 and implemented in TRANSURANUS is also implemented in GERMINAL with the same parameters.

4.1.2 Melting temperature

The correlation for thermal conductivity presented in Section 3.1.2 and implemented in TRANSURANUS is also implemented in GERMINAL with the same parameters.

The burnup correction in GERMINAL is extrapolated above the applicability upper bound (i.e. above 110 GWd/tHM), this choice being reasonable considering the asymptotical evolution of the melting temperature correlation with burnup.

4.1.3 Heat capacity

The evaluation of the heat capacity in GERMINAL implements a biphasic law that also takes into account the heat of fusion. It is expressed as follows [3]:

$$C_p = (1 - x_{liq})\, C_{p_{sol}} + x_{liq}\, C_{p_{liq}} + x_{liq}\,(1 - x_{liq})\,\frac{6L}{T_{liq} - T_{sol}} \tag{14}$$

Where, C_p is the molar heat capacity of the biphasic MOX fuel (J/mol/K); x_{liq} is the liquid fraction (dimensionless); $C_{p_{sol}}$ and $C_{p_{liq}}$ are respectively the molar heat capacity of the solid phase and the liquid phase (J/mol/K); T_{sol} and T_{liq} are the solidus and liquidus temperatures, i.e., the temperatures at the start and at the end of melting; L is the molar heat of fusion (J/mol).

This formulation verifies the conditions as follows:

$$\begin{array}{ll} \lim C_p = C_{p_{sol}} & \lim C_p = C_{p_{liq}} \\ T \longrightarrow T_{sol} & T \longrightarrow T_{liq} \\ T < T_{sol} & T < T_{liq} \\ \text{or } T > T_{sol} & \text{or } T > T_{liq} \end{array} \qquad \int_{T_{sol}}^{T_{liq}} C_p(\tau)d\tau = \frac{C_{p_{sol}} + C_{p_{liq}}}{2} \times (T_{liq} - T_{sol}) + L \tag{15}$$

It allows us to simulate transient conditions that may cause fuel melting.

A variant of this formulation was derived in GERMINAL by introducing the estimation of the melting temperature (that is to say, the solidus temperature corresponding to the start of melting) by the correlation issued from INSPYRE Deliverable D6.2_v2 and published in [7], as previously described in Section 4.1.2.

A complementary assumption was necessary to fix the estimation of the liquidus temperature, as no associated correlation was proposed for it. To do that, we retained for the temperature step $(T_{liq} - T_{sol})$ an evolution which is consistent with that described by the correlations already available in GERMINAL, that is to say:

$$T_{liq} - T_{sol} = 4 \times \Delta T_{max}^{liq-sol} \times [Pu] \times (1 - [Pu]) \tag{16}$$

This parabolic evolution with the plutonium content takes a maximum value, $\Delta T_{max}^{liq-sol}$, for a plutonium content equal to 0.5. It is underlined that this assumption is based on the analysis of previously existing correlations, but it is not supported by experimental data. As a main consequence, the simulation of transient conditions using the new law is appropriate until melting point, *but not above*. The maximum temperature step $\Delta T_{max}^{liq-sol}$ was thus introduced as an adjustable parameter.

All the other properties appearing in the formulation (i.e., $C_{p_{sol}}$, $C_{p_{liq}}$, L) are evaluated using the correlations already implemented in GERMINAL. The liquid fraction x_{liq} is an unknown of the transient thermal analysis with fuel melting.

4.2 Mechanical properties

4.2.1 Thermal expansion

The correlation for thermal expansion presented in Section 2.1 and implemented in TRANSURANUS is also implemented in GERMINAL with the same parameters. The values used for $T^{(m)}$ are the best-estimate ones.

This correlation for the thermal expansion of MOX fuel in solid phase is integrated in a biphasic law that takes into account the volume increase during melting and also evaluates the thermal expansion in liquid phase beyond melting.

4.2.2 Young's modulus

The Young's modulus correlation integrated in GERMINAL for MOX fuels is also issued from SCK.CEN work (reported in INSPYRE Deliverable D6.3 [4]) and is described in Section 2.2. However, the temperature dependency is taken into account in the same way than that previously adopted for TRANSURANUS code – cf. Section 3.2. The revised E_T (GPa) is obtained by applying to $E_{MOX}(y)$ a dimensionless weighting $f(T)/f(273\ K)$. The function $f(T)$ is given by Eq. 12.

This description of the Young's modulus dependency on temperature is fully consistent with the current state-of-the-art, especially with the outcomes of ESNII+ project (see Section 3.2).

4.3 Inert gas behaviour

The inert gas behaviour description by the SCIANTIX code [21] was integrated in GERMINAL [3]. The SCIANTIX fission gas modelling, whose development and integration in the fuel performance codes are part of the technical objectives of INSPYRE Project, is described in [36]. This section provides details about some adaptations made when introducing SCIANTIX in the calculation scheme of GERMINAL. A first feedback on the model after its integration is also presented.

SCIANTIX was integrated in GERMINAL by introducing the model for fission gas behaviour in the multi-physics convergence loop for one considered slice of the fuel pin. The updated coupling scheme is presented in the Figure 6 below. The main coupling effects induced by the fission gas behaviour are linked to the release of the gases that will modify the gas composition inside the fuel pin gap and consequently the heat transfer from the fuel pellets to the cladding. Moreover, the fuel swelling induced by the retained fission gases will also contribute to modify the heat transfer between fuel and cladding by changing the gap thickness.

The main improvements that are expected through the coupling of SCIANTIX with GERMINAL concern the simulation of the fuel pin behaviour at intermediate power level; that is irradiation conditions for which the fission gas release is not 100 % any longer, and must consequently be evaluated as precisely as possible, as well as the contribution of gas swelling to the geometrical evolution of the fuel pellet. The simulation of the behaviour at the fuel pin extremities would clearly benefit from such modelling improvements.

The coupling of SCIANTIX with GERMINAL was very easy to perform. As SCIANTIX model is written in C++ language, the creation of an interface with GERMINAL was immediate.

Then, the first calculations performed with the coupled GERMINAL/SCIANTIX suite revealed several issues that need to be solved to stabilize the model predictions in Fast Reactor conditions.

For the evaluation of the fission gas release, it is necessary to account for the evolution of the grain size (i.e., the fuel micro-structure) during irradiation. For the modelling of intra-granular behaviour, the grain boundary fixes the limit of the domain where the fission gases are diffusing – being trapped in bubbles and then re-soluted into the grain, becoming available again for diffusion. When reaching the grain boundary, the fission gases accumulate in bubbles, before being released. The size of the grain determines the time to diffuse to the grain boundary, and consequently strongly impacts the estimation of the gas release.

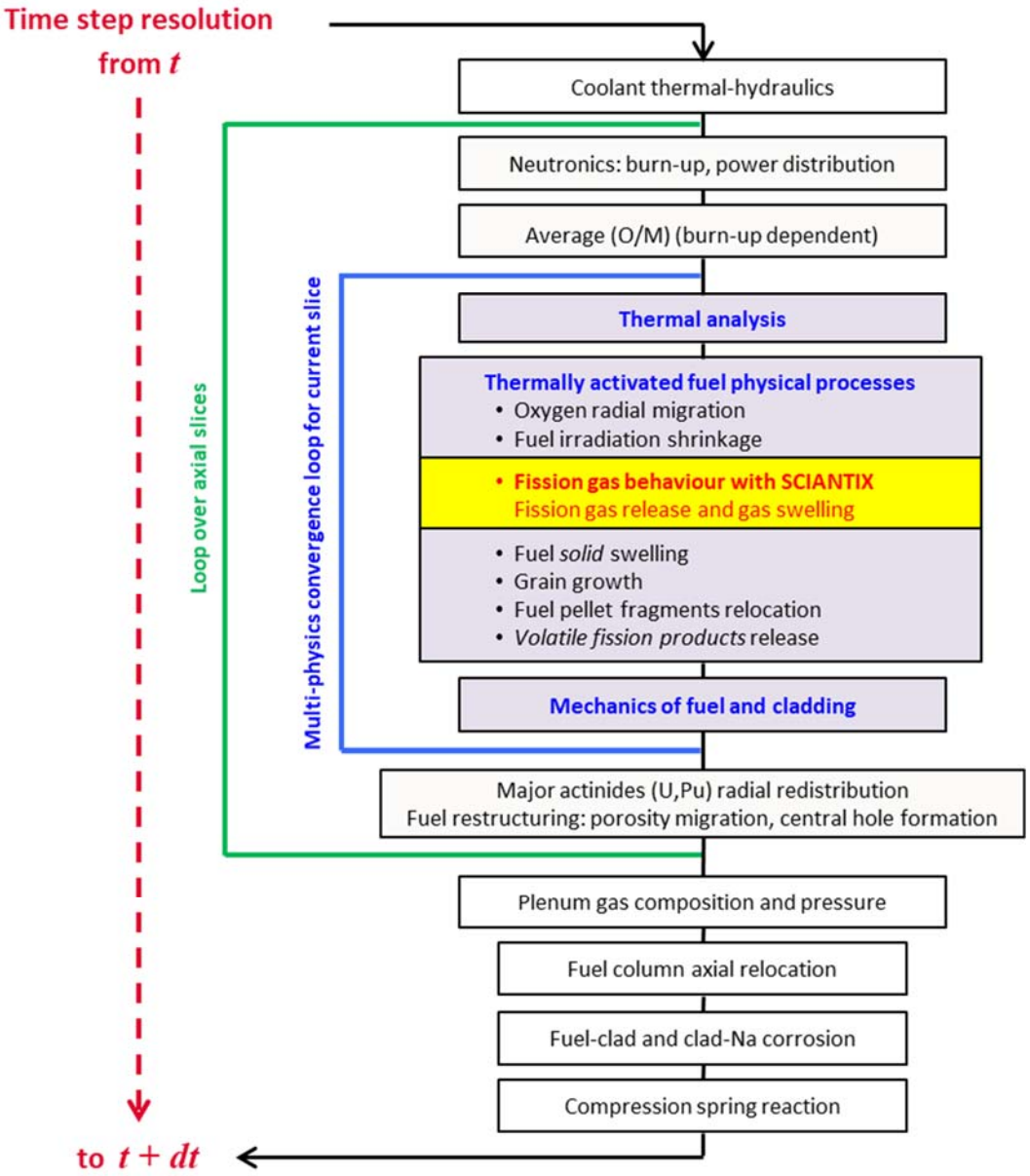

Figure 6: Single time step resolution by GERMINAL involving SCIANTIX model for fission gas behaviour.

The grain growth during irradiation is usually estimated using empirical correlations, essentially depending on temperature and time. It appears to be necessary to limit the grain growth predictions differently in the various zones of the fuel pellet, especially for the columnar grains zone, i.e., to define a maximum grain size being representative of the diameter of the columnar grains. This point appears essential to obtain predictions for gas release in agreement with observations. The possibility to define upper bounds for the grain growth in the different zones of the fuel pellets – columnar grains zone, equiaxed grain zone, un-restructured zone – was thus introduced in the interface of SCIANTIX model implemented in GERMINAL. These parameters are adjustable in the input data file and might be calibrated using experimental data.

Concerning the evaluation of the gas swelling, it is first observed that controlling the grain growth (previous point) is also necessary regarding swelling, since the envelope surface of the grain determines a “covering capacity” by inter-granular bubbles, the accumulation of which represents the main contribution to gas swelling.

The first calculations performed with the coupling of SCIANTIX with GERMINAL also revealed the necessity to control the predictions of the growth of the inter-granular bubbles. There was no asymptotical regime for the growth of the inter-granular bubbles with the original formulation of the model. As a consequence, inter-granular bubbles could grow indefinitely. A first simple solution consisting in setting a maximum bubble size at a grain boundary was introduced.

In addition, physically grounded limits were introduced in the description of the bubbles percolation at the grain boundary. This work was performed during a collaborator exchange between POLIMI and CEA in the INSPYRE Project. The estimation of the vented fraction of bubbles on the grain faces is based on a numerical random experience enabling the evaluation of the venting probability under the assumption that a bubble is vented when it is part of a collection touching at least one edge of the face. As detailed in Deliverable D6.4, the estimation is done using a sample with varying bubble numbers, sizes and distributions on the grain face. This method leads to an estimate of the vented fraction, in correlation with the bubble density on the grain face, as a function of the bubble radius. The vented fraction of bubbles is thus growing with the fractional coverage of the grain face by the bubbles (F). There is an inflection point for $F = 0.5$; and 99.9+ % of the bubbles are vented for $F = \pi/4$; the variance decreases as F increases. Based on this estimation of the vented fraction, the portion of atoms released as they get to the grain boundary increases with the fractional coverage. This allows us to describe a self-limiting bubble coalescence and growth at the grain boundary.

The results detailed in Deliverable D6.4 show the improvements brought by this new model. The models for both bubble size at grain boundary and inter-granular gas swelling are more physically-justified than the original model. The integration of this work in the latest version of SCIANTIX model is underway.

Less fundamental adaptations done while integrating the SCIANTIX models in GERMINAL are as follows.

- Resolution of the gas diffusion inside the fuel grain:
  An adapted solver handling separately the two unknowns – gas in solution in the fuel matrix and gas in bubbles – was implemented, to be used when the resolution of the equivalent diffusion equation may be indeterminate, due to null terms – especially at null power at the initial time step. The implementation of this solver was one of the first actions done during the collaborator exchange between POLIMI and CEA. The possibility to change the solver during the calculation and to use the reduced order model for the diffusion in the columnar grains zone was also introduced in the interface of SCIANTIX model implemented in GERMINAL.
- Evaluation of the gas diffusion coefficient inside the grain:
  Several options allowing one to adjust the estimation of the diffusion coefficient were introduced, i.e., the Turnbull formulation with adjustable parameters; the Arrhenius law with adjustable parameters; a prototypical formulation with a thermally activated term saturating quicker (hyperbolic tangent-shaped), also with adjustable parameters. The possibility to apply a global scaling factor on the gas diffusion coefficient was implemented as well. These options were introduced since it was noticed that the gas trapping rate by the intra-granular bubbles can become preponderant at high temperatures compared to the resolution rate. This can lead to predict gas retention in the hottest region of the fuel pellet. This is why the possibility to try different estimations of the gas diffusion coefficient was introduced. In addition, the possibility to account for a maximum diffusion coefficient in the evaluation the trapping rate was also implemented, in order to check a direct effect of limiting the trapping rate on the predictions of gas retention.

5 CONCLUSIONS

This document summarises the implementation of the new models and material properties in the fuel performance codes considered in the INSPYRE Project (MACROS, TRANSURANUS, GERMINAL,). This objective was achieved by implementing mechanistic models developed and recent data for material properties obtained in various other WPs of the INSPYRE Project, but also those available in open literature and yielded by the ESNII+ Project. In particular, we implemented in the MACROS code the new correlations for the thermal expansion coefficient (Equations 1-3) and the Young's modulus (Equations 4-7) of MOX fuels. We implemented in the TRANSURANUS code new correlations for thermal conductivity (Equations 8 and 9) and melting temperature (Equations 10 and 11) of MOX fuels, thermal expansion coefficient (Equations 1, 2 and 10), Young's modulus (Equations 4-6, 12 and 13), properly considering the most relevant parameters. Finally, we implemented new correlations for thermal conductivity (Equations 8 and 9), melting temperature (Equations 10 and 11), heat capacity (Equations 14 to 16), thermal expansion (Equations 1-3) and Young's modulus (Equations 4-6, 12 and 13) in the GERMINAL code.

For the fission gas behaviour, the specific intermediate-scale code SCIANTIX was developed at POLIMI. It includes mechanistic models for both the helium behaviour as well as the high burnup structure formation and its influence on the fission gas behaviour. The SCIANTIX code is open source and was coupled with the GERMINAL and TRANSURANUS codes, albeit with minor adaptations for each code.

Finally, the new versions of the fuel performance codes developed in the INSPYRE Project and outlined in this document need to be assessed. This will be performed by simulating the behaviour of several rods during irradiation experiments SUPERFACT-1, NESTOR-3, and RAPSODIE-I and will be presented in Deliverable D7.3 of the INSPYRE project.

REFERENCES

1. Lemehov, S.E., *et al.*, *MACROS benchmark calculations and analysis of fission gas release in MOX with high content of plutonium.* Progress in Nuclear Energy, 2012. 57: p. 117-124.
2. Lassmann, K. and A. Moreno, *The Light-Water-Reactor-Version of the URANUS Integral Fuel-Rod Code.* Atomkernenergie, 1977(Bd. 30, Lfg. 3): p. 207-215.
3. Lainet, M., *et al.*, *GERMINAL, a fuel performance code of the PLEIADES platform to simulate the in-pile behaviour of mixed oxide fuel pins for sodium-cooled fast reactors.* Journal of Nuclear Materials, 2019. 516: p. 30-53.
4. Lemehov, S., *New correlations of thermal expansion and Young's modulus based on existing literature and new data*, in *INSPYRE project deliverables*, M. Bertolus, Editor. 2020: Brussels, Belgium.
5. Martin, D.G., *The thermal expansion of solid UO_2 and (U,Pu) mixed oxides — a review and recommendations.* Journal of Nuclear Materials, 1988. 152(2): p. 94-101.
6. Magni, A., *et al.*, *Report on the improved models of melting temperature and thermal conductivity for MOX fuels and JOG*, in *INSPYRE project deliverables*, M. Bertolus, Editor. 2020: Brussels, Belgium.
7. Magni, A., *et al.*, *Modelling and assessment of thermal conductivity and melting behaviour of MOX fuel for fast reactor applications.* Journal of Nuclear Materials, 2020. 541: p. 152410.
8. Hirooka, S. and M. Kato, *Sound speeds in and mechanical properties of $(U,Pu)O_{2-x}$.* Journal of Nuclear Science and Technology, 2018. 55(3): p. 356-362.
9. *SCDAP/RELAP5/MOD3.3 Code Manual MATPRO - a library of material properties for light-water-reactor accident analysis*. 2000, USNRC.
10. Ottaviani, J.P., *et al.*, *State of the art with a literature review of MOX fuel properties*, E. project, Editor. 2015, European Commission. p. 143.
11. Balboa, H., *et al.*, *Assessment of empirical potential for MOX nuclear fuels and thermomechanical properties.* Journal of Nuclear Materials, 2017. 495: p. 67-77.
12. Padel, A. and Ch. De Novion, *Constantes elastiques des carbures, nitrures et oxydes d'uranium et de plutonium* Journal of Nuclear Materials, 1969. 33: p. 40-51.
13. Cooper, M.W.D., M.J.D. Rushton, and R.W. Grimes, *A many-body potential approach to modelling the thermomechanical properties of actinide oxides.* Journal of Physics: Condensed Matter, 2014. 26(10): p. 105401.
14. Gibby, R.L., *Thermal expansion of mixed oxide fuel*. 1974.
15. Pizzocri, D., *et al.*, *Report describing the complete inert gas behaviour model with grain recrystallization and the corresponding improved data*, in *INSPYRE project deliverables*, M. Bertolus, Editor. 2020: Brussels, Belgium.
16. Baker, C., *The fission gas bubble distribution in uranium dioxide from high temperature irradiated SGHWR fuel pins.* Journal of Nuclear Materials, 1977. 66: p. 283-291.
17. Barani , T., *Mechanistic modeling of fission gas behavior in conventional and advanced nuclear fuel*, in *Politecnico di Milano, Italy*. 2020: Milano, Italy.
18. Barani, T., *et al.*, *Modeling intra-granular fission gas bubble evolution and coarsening in uranium dioxide during in-pile transients.* Journal of Nuclear Materials, 2020. 538: p. 152195.
19. Baker, C. and J.C. Killeen. *Fission gas release during post irradiation annealing of UO_2*. in *International Conference on Materials for Nuclear Reactor Core Applications, Bristol, United Kingdom, October 27--29, 1987*.
20. Killeen, J.C. and C. Baker. *Fission gas release during post irradiation annealing of UO_2 up to 1750°C*. in *Topical Meeting on LWR Fuel Performance*. 1985. Orlando, Florida, USA: ANS.

21. Small, G.J. *Bubble development and fission gas release during rapid heating of 18 GWd/TeU UO_2*. in *Specialists Meeting of Fission Product Release and Transport in Gas-Cooled Reactors*. 1985. Berkeley, United Kingdom: International Atomic Energy Agency.
22. White, R.J., R.C. Corcoran, and J.P. Barnes, *A Summary of Swelling Data Obtained from the AGR/ Halden Ramp Test Programme*. 2006.
23. Pizzocri, D., *et al.*, *A model describing intra-granular fission gas behaviour in oxide fuel for advanced engineering tools.* Journal of Nuclear Materials, 2018. 502: p. 323-330.
24. *International Fuel Performance Experiments (IFPE) Database*. 2018; Available from: http://www.nea.fr/html/science/fuel/ifpelst.html.
25. Noirot, J., *et al.*, *Post-irradiation examinations and high-temperature tests on undoped large-grain UO_2 discs.* Journal of Nuclear Materials 2015. 462: p. 77-84.
26. Gerczak, T.J., *et al.*, *Restructuring in high burnup UO_2 studied using modern electron microscopy.* Journal of Nuclear Materials, 2018. 509: p. 245-259.
27. Barani, T., *et al.*, *Modeling high burnup structure in oxide fuels for application to fuel performance codes. part I: High burnup structure formation.* Journal of Nuclear Materials, 2020. 539: p. 152296.
28. Barani , T., *Sviluppo del codice di comportamento dei gas di fissione SCIANTIX per l'analisi del combustibile ossido nucleare in transitori ad alte temperature e ad alti tassi di bruciamento*. 2020, Politecnico di Milano: Milano. p. 11.
29. Cognini, L., *et al.*, *Towards a meso-scale mechanistic description of intra-granular helium behaviour in oxide fuel for application in fuel performance codes.* Nuclear Engineering and Technology, 2020: submitted.
30. Cognini, L., *et al.*, *Helium solubility in oxide nuclear fuel: Derivation of new correlations for Henry's constant.* Nuclear Engineering and Design, 2018. 340: p. 240–244.
31. Luzzi, L., *et al.*, *Helium diffusivity in oxide nuclear fuel: Critical data analysis and new correlations.* Nuclear Engineering and Design, 2018. 330: p. 265–271.
32. Van Brutzel, L. and A. Chartier, *A new equation of state for helium nanobubbles embedded in UO_2 matrix calculated via molecular dynamics simulations.* Journal of Nuclear Materials, 2019. 518: p. 431-439.
33. Van Uffelen, P., *et al.*, *An experimental study of grain growth in mixed oxide samples with various microstructures and plutonium concentrations.* Journal of Nuclear Materials, 2013. 434: p. 287-290.
34. Talip, Z., *et al.*, *Thermal diffusion of Helium in ^{238}Pu-doped UO_2.* Journal of Nuclear Materials, 2014. 445(1-3): p. 117-127.
35. Veshchunov, M.S., *et al.*, *Development of the mechanistic code MFPR for modelling fission-product release from irradiated UO_2 fuel.* Nuclear Engineering and Design, 2006. 236: p. 179-200.
36. Pizzocri, D., T. Barani, and L. Luzzi, *SCIANTIX: A new open source multi-scale code for fission gas behaviour modelling designed for nuclear fuel performance codes.* Journal of Nuclear Materials, 2020. 532: p. 152042.
37. Pizzocri, D., T. Barani , and L. Luzzi, *Coupling of TRANSURANUS with the SCIANTIX fission gas behaviour module*, in *International Workshop "Towards nuclear fuel modelling in the various reactor types across Europe"*, JRC, Editor. 2019: Karlsruhe, Germany.
38. Rufeh, F., D.R. Olander, and T.H. Pigford, *The solubility of helium in uranium dioxide.* Nuclear Science and Engineering, 1965. 23: p. 335-338.
39. Olander, D.R., *Theory of Helium Dissolution in Uranium Dioxide. II. Helium Solubility.* The Journal of Chemical Physics, 1965. 43(3): p. 785-788.
40. Maugeri, E., *et al.*, *Helium solubility and behaviour in uranium dioxide.* Journal of Nuclear Materials, 2009. 385(2): p. 461-466.
41. Lassmann, K., *et al.*, *The radial distribution of plutonium in high burnup UO_2 fuels.* Journal of Nuclear Materials, 1994. 208(3): p. 223-231.

42. Lassmann, K., C.T. Walker, and J. van de Laar, *Extension of the TRANSURANUS burnup model to heavy water reactor conditions.* Journal of Nuclear Materials, 1998. 255(2-3): p. 222-233.
43. Schubert, A., *et al.*, *Extension of the TRANSURANUS burn-up model.* Journal of Nuclear Materials, 2008. 376: p. 1-10.
44. Pizzocri, D., *et al.*, *Modeling of the grain-boundary vented fraction for the description of fission gas behaviour in fast reactor conditions.* in preparation for Journal of nuclear materials, 2020.
45. Barani , T., *et al.*, *Development of a reduced order model of fission gas diffusion in columnar grains*, in *NuFuel 2017 Workshop*. 2017: Lecco, Italy.